Biochemical and Biophysical Research Communications 443 (2014) 126–131

Contents lists available at ScienceDirect

Biochemical and Biophysical Research Communications

journal homepage: www.elsevier.com/locate/ybbrc

Peptides derived from human galectin-3 N-terminal tail interact with its carbohydrate recognition domain in a phosphorylation-dependent manner

M. Álvaro Berbís [a], Sabine André [b], F. Javier Cañada [a], Rüdiger Pipkorn [c], Hans Ippel [d,e], Kevin H. Mayo [e], Dieter Kübler [f], Hans-Joachim Gabius [b], Jesús Jiménez-Barbero [a,*]

[a] Chemical and Physical Biology Department, Centro de Investigaciones Biológicas, CSIC, 28040 Madrid, Spain
[b] Institute of Physiological Chemistry, Faculty of Veterinary Medicine, Ludwig-Maximilians University, 80539 Munich, Germany
[c] Central Peptide Synthesis Unit, German Cancer Research Center, 69120 Heidelberg, Germany
[d] Department of Biochemistry, CARIM, University of Maastricht, Maastricht, The Netherlands
[e] Department of Biochemistry, Molecular Biology and Biophysics, University of Minnesota, Minneapolis, MN 55455, USA
[f] Biomolecular Interactions, German Cancer Research Center, 69120 Heidelberg, Germany

ARTICLE INFO

Article history:
Received 12 November 2013
Available online 22 November 2013

Keywords:
Agglutinin
Collagen
Lectin
Phosphopeptide
Phosphorylation

ABSTRACT

Galectin-3 (Gal-3) is a multi-functional effector protein that functions in the cytoplasm and the nucleus, as well as extracellularly following non-classical secretion. Structurally, Gal-3 is unique among galectins with its carbohydrate recognition domain (CRD) attached to a rather long N-terminal tail composed mostly of collagen-like repeats (nine in the human protein) and terminating in a short non-collagenous terminal peptide sequence unique in this lectin family and not yet fully explored. Although several Ser and Tyr sites within the N-terminal tail can be phosphorylated, the physiological significance of this post-translational modification remains unclear. Here, we used a series of synthetic (phospho)peptides derived from the tail to assess phosphorylation-mediated interactions with ^{15}N-labeled Gal-3 CRD. HSQC-derived chemical shift perturbations revealed selective interactions at the backface of the CRD that were attenuated by phosphorylation of Tyr 107 and Tyr 118, while phosphorylation of Ser 6 and Ser 12 was essential. Controls with sequence scrambling underscored inherent specificity. Our studies shed light on how phosphorylation of the N-terminal tail may impact on Gal-3 function and prompt further studies using phosphorylated full-length protein.

1. Introduction

The members of the galectin family are potent effectors in diverse cellular mechanisms such as growth regulation or motility, by virtue of glycan or protein recognition acting inside the cell, at the cell surface and extracellularly [1–3]. In structural aspects, the modular design of galectin-3 (Gal-3) is unique. It is composed of the common β-sandwich-type carbohydrate recognition domain (CRD) linked to collagen-like repeats (nine in human Gal-3) and an N-terminal 12-mer peptide with two sites for serine phosphorylation, the explanation why Gal-3 is called a chimera-type galectin [4,5]. Since every animal species studied so far harbors Gal-3 despite marked inter-species differences in the total number of galectin genes and the sequences in the two non-CRD regions appear conserved [4–7], the trimodular structure likely bears special physiological significance.

At present, the non-CRD portion is implicated in non-classical secretion [1,8,9]; serine phosphorylation of the starting peptide (at S6 and S12 [9–11]) is known to play a role in nuclear export [1,13,14]. Although an impact on binding lactose, ganglioside GM1 and N-glycans was excluded [12,15,16], this phosphorylation reduced Gal-3 reactivity to laminin and asialomucin but enhanced both complex formation with the cell adhesion molecule L1 and its association with Thy-1-rich microdomains in neurons [17,18]. Equally intriguing, tyrosine phosphorylation by non-receptor kinases cAbl/Arg (at Y79, Y107 and Y118 [18–20]) appears to establish a routing signal for Gal-3 to reach the cell periphery with ensuing secretion in mouse embryonic fibroblasts [21]. It is an open question whether intramolecular recognition, influenced by the status of phosphorylation, may contribute to the structural basis of these processes.

Abbreviations: CRD, carbohydrate recognition domain; Gal-3, galectin-3; HSQC, heteronuclear single-quantum coherence; NMR, nuclear magnetic resonance.

* Corresponding author.
E-mail address: jjbarbero@cib.csic.es (J. Jiménez-Barbero).

0006-291X/$ - see front matter © 2013 Elsevier Inc. All rights reserved.
http://dx.doi.org/10.1016/j.bbrc.2013.11.063

Of note, the N-terminal portion appears rather flexible, although the transition temperature at 39 °C during thermal denaturation and the bimodal charge distribution in nano-ESI mass spectrometry provide evidence for an interconverting mixture of conformers, tentatively between extended and compact forms [22,23]. Importantly, chemical shift analysis of hamster Gal-3 suggested the presence of transient contacts with the CRD, for residues in the first part of the N-terminal tail (F5, W22, W26) and L109 [24]. The delineation of a nuclear export signal, probably interacting with a transporter such as nucleoporin Nup98 [25], in the distal section of the CRD, i.e. around 240–255 in murine Gal-3 [26], in conjunction with these NMR-based observations and the switch-like impact of serine phosphorylation on nuclear export noted above, raises the intriguing possibility that serine phosphorylation can trigger so far unknown structural consequences, directly and/or indirectly. On this basis, we have tested the hypothesis of the existence of interactions with synthetic peptides and ^{15}N-labeled CRD. Looking at secretion, tyrosine phosphorylation may play into this process by favoring a conformer, most suitably in extended form to make the tail fully accessible. Testing potential for peptide – CRD reactivity followed the described strategy. To complete this study line, we have also examined the chemical shift properties of the CRD in the presence of peptides comprising one and two collagen-like repeats.

2. Materials and methods

2.1. Gal-3

Gal-3 CRD was recombinantly produced with [^{15}N]NH_4Cl as medium additive, purified by affinity chromatography on lactosylated Sepharose 4B as crucial step, and routinely checked for purity and activity as described [12,27,28].

2.2. Peptides

The peptides (sequences shown in Fig. 1) were synthesized in an automated multiple synthesizer Syro II (MultiSyn Tech, Germany) with Fmoc chemistry under atmospheric conditions at room temperature using HMPB-ChemMatrix® resins. For amino acid coupling, a fivefold excess of the Fmoc-protected amino acid was activated *in situ* with five equivalents 2-(1H-benzotriazole-1-yl)-1,1,3,3-tetramethyluronium hexafluorophosphate and DIPEA (0.5 M) in DMF. The coupling time was 40 min. The Fmoc-group was cleaved with piperidine (20%) in DMF for periods of 3 min and 10 min. After each step, the resin was washed five times with DMF. After completion of the synthesis, the resin was washed three times with DMF, dichloromethane and finally isopropanol, then dried. The following release of the peptide from the resin and of the side-chain protecting groups was performed with trifluoroacetic acid (95%), as scavenger triethylsilan/water (2.5%/2.5%) for 2.5 h at room temperature was used.

The resulting material was purified by preparative HPLC on a Kromasil 100–10C 18 μm reverse phase column (30′ × 250 mm) using an eluent of 0.1% trifluoroacetic acid in water (A) and 80% acetonitrile in water (B). Peptide was eluted with a successive linear gradient of 10% B to 80% B in 30 min at a flow rate of 23 ml/min. The fractions containing the purified peptide were lyophilized. The resulting material was characterized by analytical HPLC (Shimadzu) and MS (Thermo Finnigan LCQ).

2.3. NMR spectroscopy

All experiments were performed at 298 K in a Bruker AVANCE 600 MHz spectrometer equipped with a cryogenically-cooled z-gradient triple resonance probe. Samples for ^{1}H–^{15}N HSQC

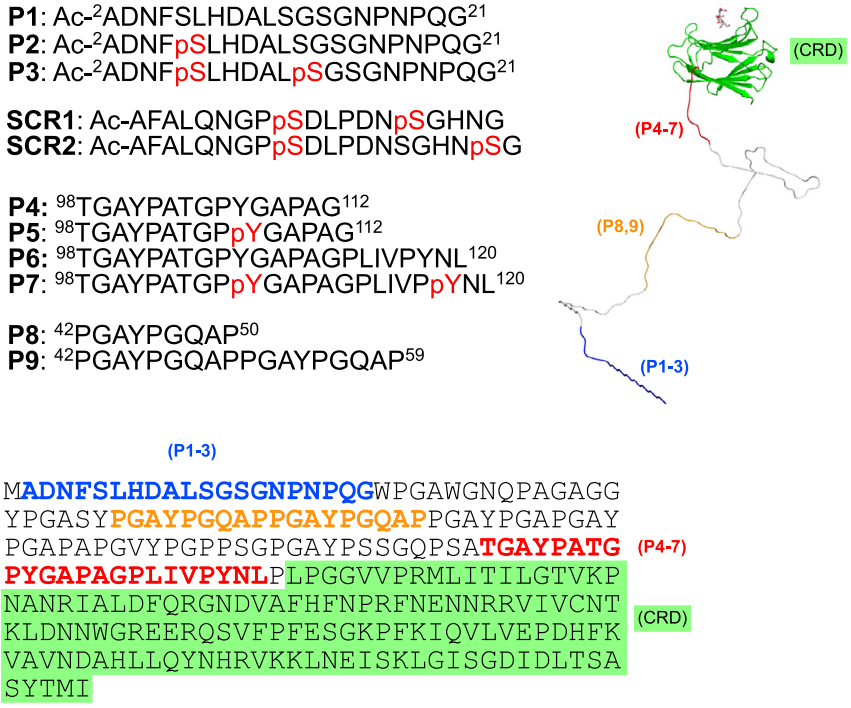

Fig. 1. Top panel: sequences of the synthetic peptides used in this study, with phosphoserine (pS) and phosphotyrosine (pY) residues highlighted in red. Bottom panel: location of the peptides in the whole protein sequence. Blue: peptides P1–P3; orange: peptides P8 and P9; blue: peptides P4–P7. The sequence of the CRD is indicated on a green background. On the right, a schematic representation of the crystal structure of the Gal-3 CRD (green), with a tail representing the N-terminal tail (at scale) is shown, with colors indicating the distribution of the studied peptides along the tail sequence. (For interpretation of the references to color in this figure legend, the reader is referred to the web version of this article.)

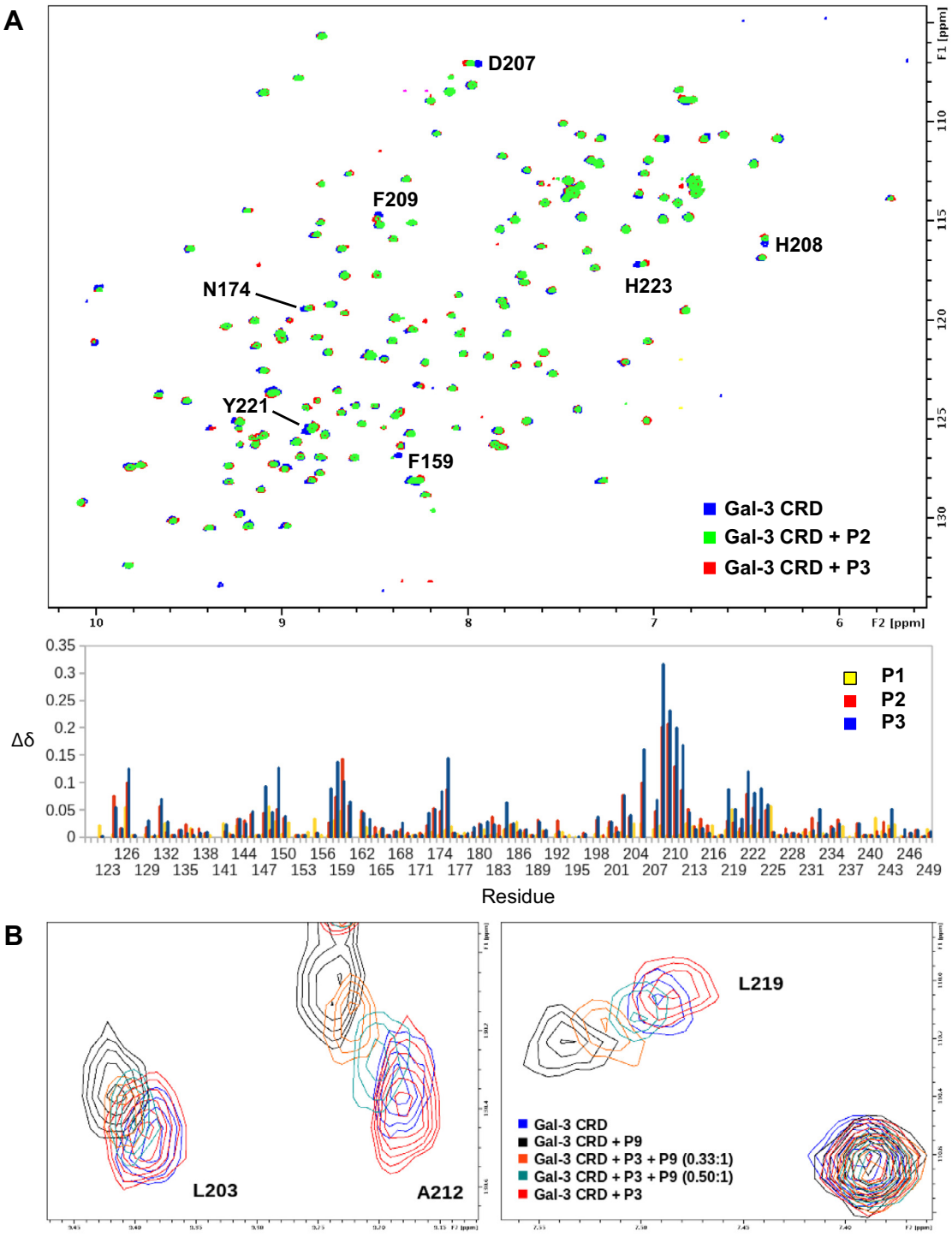

Fig. 2. (A) Top panel: superimposition of $^{1}H–^{15}N$ HSQC spectra of the Gal-3 CRD, in the absence (blue) and in the presence of ten equivalents of the N-terminal phosphopeptides P2 (green) or P3 (red), with labels indicating some of the most perturbed signals. Bottom panel: $^{1}H–^{15}N$-weighted chemical shift differences ($\Delta\delta$) for Gal-3 CRD backbone NH signals upon addition of 10 equivalents P1 (yellow), P2 (red) or P3 (blue). (B) Competition experiment showing the displacement of P9 by the addition of increasing amounts of the N-terminal phosphopeptide P3. The figure shows a superimposition of $^{1}H–^{15}N$ HSQC spectra of the Gal-3 CRD with different P9/P3 ratios. Blue: Gal-3 alone; black: in the presence of ten equivalents of P9; orange: after the addition of 3.3 equivalents of P3; green: after the addition of 5 equivalents of P3; red: in the presence of ten equivalents of P3. (For interpretation of the references to color in this figure legend, the reader is referred to the web version of this article.)

experiments contained ^{15}N-labeled human Gal-3 CRD at a concentration of 200 μM, with or without ten equivalents of the tested peptides, in PBS buffer in 90% H_2O/10% D_2O. Chemical shift perturbations were monitored using the sequence-specific assignments for the human Gal-3 CRD ^{1}H and ^{15}N resonances previously reported [29].

3. Results

3.1. Definition of peptides

To assess interactions between the Gal-3 CRD and N-terminal tail, we used $^{1}H–^{15}N$ HSQC experiments and three sets of

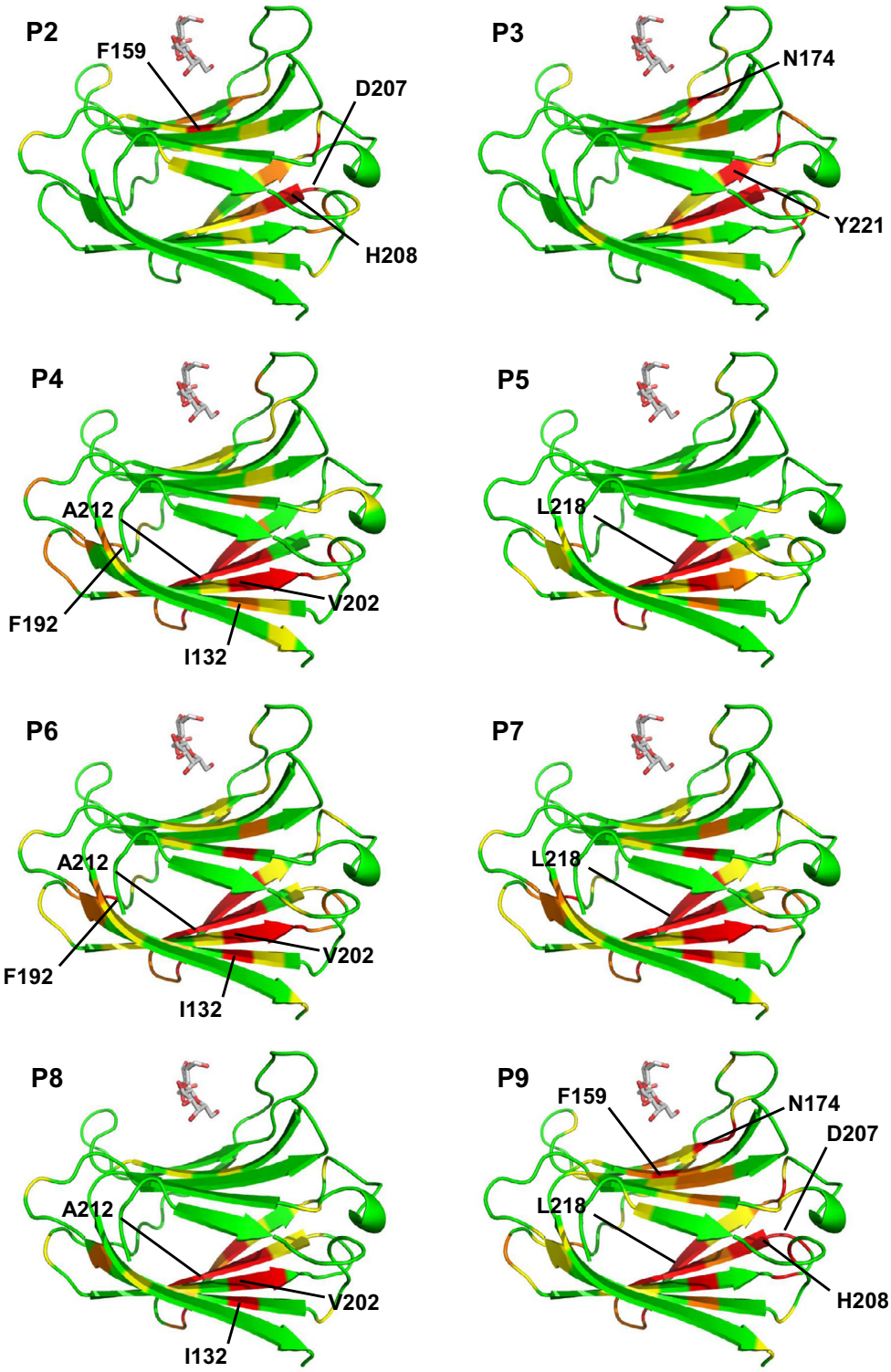

Fig. 3. Mapping of the Gal-3 CRD residues with the most shifted signals for peptides P2–P9. In all cases, the structure of the LacNAc-loaded human Gal-3 CRD (PDB: 1A3K) is shown, with residues highlighted in red for the most shifted resonances, followed by orange and yellow. (For interpretation of the references to color in this figure legend, the reader is referred to the web version of this article.)

structurally-relevant tail-derived peptides as shown in Fig. 1. The first set (P1–P3) represents the N-terminal peptide with and without Ser phosphorylation. The second set (P4–P7) encompasses sequences from the C-terminal part of the tail that contains phosphorylation sites Y107 and Y118. In the third set, we tested two peptides (P8, P9) from the collagen-like part of the tail.

3.2. N-terminal peptides

Although peptide P1 failed to show significant interactions with the CRD, its phosphorylated counterparts did (Figs. 2 and S1). Here, we found that the most markedly shifted resonances belonged to residues located at the backside of the lectin opposite to the

canonical sugar-binding site (Fig. 3), which in turn leaves the β-galactoside (e.g. lactose) binding site unaffected. Significant chemical shift perturbations of NH cross peaks belonging to residues 207–211 suggests that K210 is a likely contact site for phosphate groups within the tail.

The use of two scrambled control phosphopeptides (SCR1 and SCR2) allowed us to conclude that these effects were specific. Despite the presence of two phosphate groups in SCR2, the NMR spectra of Gal-3 CRD showed only very small chemical shift perturbations (Fig. S2). When the distance between the two phosphates was maintained as in SCR1, some minor chemical shift perturbations were observed (Fig. S3), but not to the extent observed with the non-scrambled peptide. Overall, these results strongly suggest that the N-terminal peptide of human Gal-3 can specifically interact with the CRD in a phosphorylation-dependent and sequence-specific manner.

3.3. Tyr-P peptides

Phosphorylation of Tyr 107 and Tyr 118 had the opposite effect. Whereas peptides P4–P7 elicited significant chemical shift perturbations of resonances from the CRD (Figs. 4 and S4), their phosphorylated counterparts actually attenuated interactions with the CRD. Once again, the most highly shifted signals belonged to residues located at the backside of the β-sandwich structure (Fig. 3), and chemical shift differences were generally greater with the longer peptides P6 and P7. In any event, phosphorylation decreased the extent of chemical shift perturbations in the Gal-3 CRD, indicating that affinity of these phosphorylated peptides towards the CRD is significantly reduced. Thus, phosphorylation of serine and tyrosine residues within the N-terminal tail appears to modulate interactions with the CRD differentially.

3.4. Pro/Gly-rich tandem-repeat peptides

To complete the study, we tested peptides containing one and two repeat sequences derived also from the tail, specifically one peptide comprising residues 42–50 (P8) and another comprising residues 42–59 (P9). The observed chemical shift perturbations within the CRD were rather similar compared to those exerted by peptides P4–P7, consistent with their sequence similarity (Figs. 3 and S5). The profile of apparent contacts suggests that the region of interaction is somewhat larger for P9 than for the single-repeat variant peptide P8.

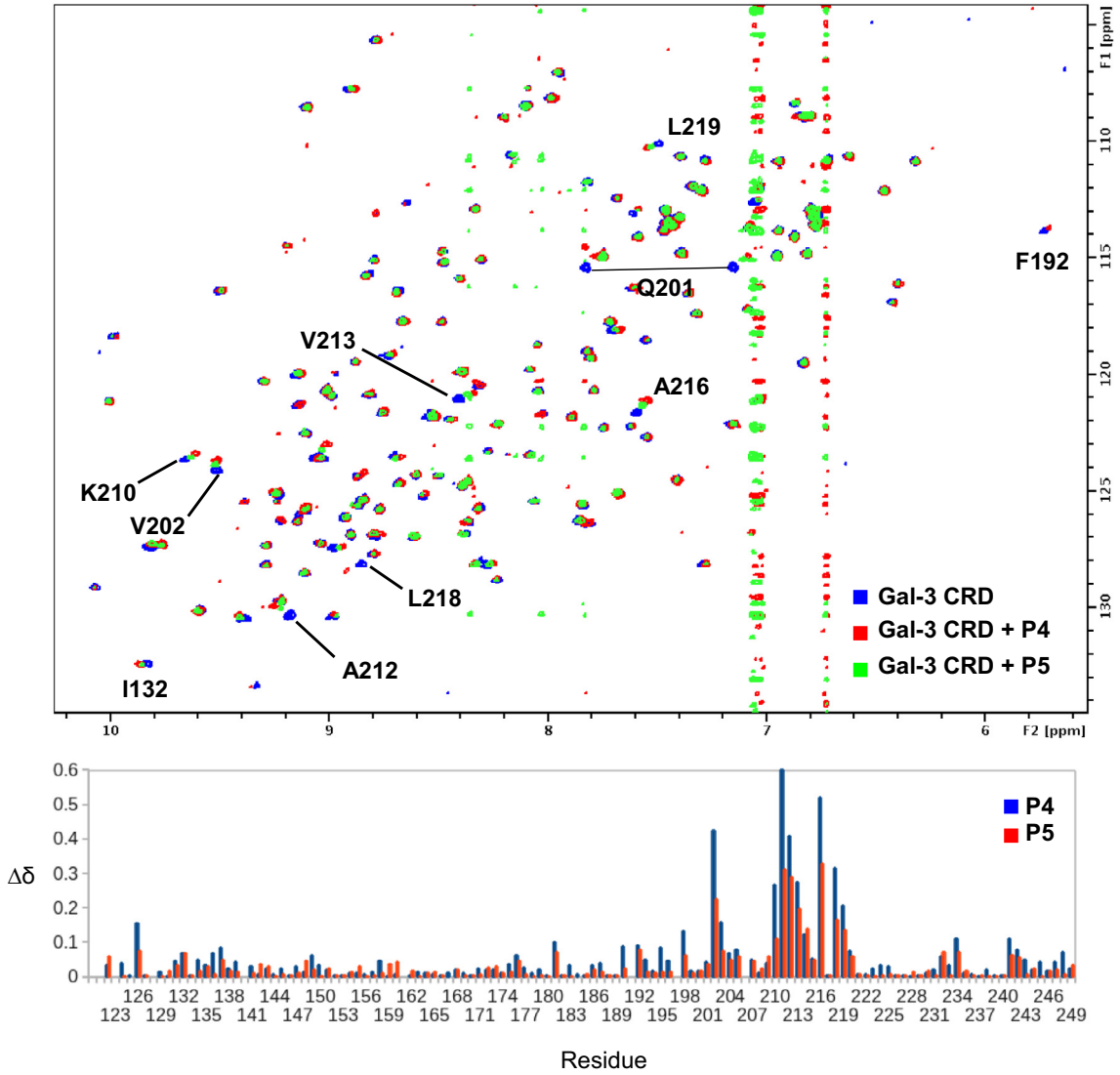

Fig. 4. Top panel: superimposition of $^{1}H–^{15}N$ HSQC spectra of the Gal-3 CRD, in the absence (blue) and in the presence of ten equivalents of P4 (red) or P5 (green). Bottom panel: $^{1}H–^{15}N$-weighted chemical shift differences (Δδ) for Gal-3 CRD backbone NH signals upon addition of 10 equivalents P4 (blue) or P5 (red). (For interpretation of the references to color in this figure legend, the reader is referred to the web version of this article.)

Because many of these peptides appeared to interact with the same region of the Gal-3 CRD, we performed a competition experiment to see whether phosphorylated N-terminal peptide P3 could displace peptide P9 from the CRD. The results of this experiment are illustrated in Fig. 2B, that focuses on three signals (L203, A212 and L219) which are significantly perturbed by the presence of P9, but not by that of P3. Addition of increasing amounts of P3 to the sample of Gal-3 CRD + P9 reversed the chemical shift changes induced by the presence of P9, thus indicating that N-terminal phosphopeptide P3 can compete with the two tandem-repeat peptide P9 for binding to the CRD. These evidences suggest that phosphorylation of Gal-3 at the N-terminus may alter the Gal-3 structure, potentially with recognition and/or functional consequences.

4. Discussion

Interaction of the Gal-3 CRD with synthetic (phospho)peptides derived from its N-terminal tail has been assessed using NMR HSQC experiments with ^{15}N-labeled CRD. Results show that distinct N-terminal peptides can interact at specific sites within the Gal-3 CRD, suggesting that a similar behavior may take place with full length Gal-3. Thus, the reported data can be relevant for association of tail-derived peptides (by proteolytic truncation of Gal-3) with the lectin, as well as for intra- and intermolecular interactions, the latter in Gal-3 aggregates formed with multivalent ligands. Moreover, while phosphorylation of Ser 6 and Ser 12 in specific N-terminal peptides promotes association with the CRD, phosphorylation of Y107 and Y118 in other peptides attenuates this association. In this regard, serine and tyrosine phosphorylation of the N-terminal tail may act as on/off switches or modulators for various functions of Gal-3.

These results give respective experiments on the level of the full-length protein a clear direction, herein then analyzing unsubstituted and phosphorylated proteins as well as variants with shortened tails, in the absence and presence of glycoclusters.

Acknowledgments

We gratefully acknowledge the financial support by MINECO of Spain (Grant CTQ2012-32025) and Comunidad de Madrid (MHit project) as well as the EC-funded BM1003 and CM1102 COST actions, the GlycoHIT program (contract No. 260600) and the GLYCOPHARM ITN project. M.A.B. acknowledges a FPI Ph.D. fellowship from the Spanish Ministry of Economy and Competitiveness.

Appendix A. Supplementary data

Supplementary data associated with this article can be found, in the online version, at http://dx.doi.org/10.1016/j.bbrc.2013.11.063.

References

[1] K.C. Haudek, K.J. Spronk, P.G. Voss, R.J. Patterson, J.L. Wang, E.J. Arnoys, Dynamics of galectin-3 in the nucleus and cytoplasm, Biochim. Biophys. Acta 2010 (1800) 181–189.
[2] H.J. Gabius, S. André, J. Jiménez-Barbero, A. Romero, D. Solís, From lectin structure to functional glycomics: principles of the sugar code, Trends Biochem. Sci. 36 (2011) 298–313.
[3] K. Smetana Jr., S. André, H. Kaltner, J. Kopitz, H.J. Gabius, Context-dependent multifunctionality of galectin-1: a challenge for defining the lectin as therapeutic target, Expert Opin. Ther. Targets 17 (2013) 379–392.
[4] K. Kasai Jr., J. Hirabayashi, Galectins: a family of animal lectins that decipher glycocodes, J. Biochem. 119 (1996) 1–8.
[5] D.N.W. Cooper, Galectinomics: finding themes in complexity, Biochim. Biophys. Acta 1572 (2002) 209–231.
[6] H. Kaltner, D. Kübler, L. López-Merino, M. Lohr, J.C. Manning, M. Lensch, J. Seidler, W.D. Lehmann, S. André, D. Solís, H.J. Gabius, Toward comprehensive analysis of the galectin network in chicken: unique diversity of galectin-3 and comparison of its localization profile in organs of adult animals to the other four members of this lectin family, Anat. Rec. 294 (2011) 427–444.
[7] H. Kaltner, H.J. Gabius, A toolbox of lectins for translating the sugar code: the galectin network in phylogenesis and tumors, Histol. Histopathol. 27 (2012) 397–416.
[8] H.C. Gong, Y. Honjo, P. Nangia-Makker, V. Hogan, N. Mazurak, R.S. Bresalier, A. Raz, The NH_2 terminus of galectin-3 governs cellular compartmentalization and functions in cancer cells, Cancer Res. 59 (1999) 6239–6245.
[9] R.P. Menon, R.C. Hughes, Determinants in the N-terminal domains of galectin-3 for secretion by a novel pathway circumventing the endoplasmic reticulum–Golgi complex, Eur. J. Biochem. 264 (1999) 569–576.
[10] E.A. Cowles, N. Agrwal, R.L. Anderson, J.L. Wang, Carbohydrate-binding protein 35. Isoelectric points of the polypeptide and a phosphorylated derivative, J. Biol. Chem. 265 (1990) 17706–17712.
[11] M.E. Hufleijt, C.W. Turck, R. Lindstedt, S.H. Barondes, H. Leffler, L-29, a soluble lactose-binding lectin, is phosphorylated on serine 6 and serine 12 *in vivo* and by casein kinase I, J. Biol. Chem. 268 (1993) 26712–26718.
[12] D. Kübler, C.W. Hung, T.K. Dam, J. Kopitz, S. André, H. Kaltner, M. Lohr, J.C. Manning, L. He, H. Wang, A. Middelberg, C.F. Brewer, J. Reed, W.D. Lehmann, H.J. Gabius, Phosphorylated human galectin-3: facile large-scale preparation of active lectin and detection of structural changes by CD spectroscopy, Biochim. Biophys. Acta 1780 (2008) 716–722.
[13] Y.G. Tsay, N.Y. Lin, P.G. Voss, R.J. Patterson, J.L. Wang, Export of galectin-3 from nuclei of digitonin-permeabilized mouse 3T3 fibroblasts, Exp. Cell Res. 252 (1999) 250–261.
[14] Y. Takenaka, T. Fukumori, T. Yoshii, N. Oka, H. Inohara, H.R.C. Kim, R.S. Bresalier, A. Raz, Nuclear export of phosphorylated galectin-3 regulates its antiapoptotic activity in response to chemotherapeutic drugs, Mol. Cell. Biol. 24 (2004) 4395–4406.
[15] P. Szabo, T.K. Dam, K. Smetana Jr., B. Dvoránková, D. Kübler, C.F. Brewer, H.J. Gabius, Phosphorylated human lectin galectin-3: analysis of ligand binding by histochemical monitoring of normal/malignant squamous epithelia and by isothermal titration calorimetry, Anat. Histol. Embryol. 38 (2009) 68–75.
[16] F.A. Habermann, S. André, H. Kaltner, D. Kübler, F. Sinowatz, H.J. Gabius, Galectins as tools for glycan mapping in histology: comparison of their binding profiles to the bovine zona pellucida by confocal laser scanning microscopy, Histochem. Cell Biol. 135 (2011) 539–552.
[17] N. Mazurek, J. Conklin, J.C. Byrd, A. Raz, R.S. Bresalier, Phosphorylation of the β-galactoside-binding protein galectin-3 modulates binding to its ligands, J. Biol. Chem. 275 (2000) 36311–36315.
[18] N. Díez-Revuelta, S. Velasco, S. André, H. Kaltner, D. Kübler, H.J. Gabius, J. Abad-Rodriguez, Phosphorylation of adhesion- and growth-regulatory human galectin-3 leads to the induction of axonal branching by local membrane L1 and ERM redistribution, J. Cell Sci. 123 (2010) 671–681.
[19] V. Balan, P. Nangia-Makker, Y.S. Jung, Y. Wang, A. Raz, Galectin-3: a novel substrate for c-Abl kinase, Biochim. Biophys. Acta 2010 (1803) 1198–1205.
[20] X. Li, Q. Ma, J. Wang, X. Liu, Y. Yang, H. Zhao, Y. Wang, Y. Jin, J. Zeng, J. Li, L. Song, P. Li, X. Qian, C. Cao, C-Abl and Arg tyrosine kinases regulate lysosomal degradation of the oncoprotein Galectin-3, Cell Death Differ. 17 (2010) 1277–1287.
[21] S. Menon, C.M. Kang, K.A. Beningo, Galectin-3 secretion and tyrosine phosphorylation is dependent on the calpain small subunit, Calpain 4, Biochem. Biophys. Res. Commun. 410 (2011) 91–96.
[22] N. Agrwal, Q. Sun, S.Y. Wang, J.L. Wang, Carbohydrate-binding protein 35. I. Properties of the recombinant polypeptide and the individuality of the domains, J. Biol. Chem. 268 (1993) 14932–14939.
[23] J. Kopitz, S. André, C. von Reitzenstein, K. Versluis, H. Kaltner, R.J. Pieters, K. Wasano, I. Kuwabara, F.T. Liu, M. Cantz, A.J.R. Heck, H.J. Gabius, Homodimeric galectin-7 (p53-induced gene 1) is a negative growth regulator for human neuroblastoma cells, Oncogene 22 (2003) 6277–6288.
[24] B. Birdsall, J. Feeney, I.D. Burdett, S. Bawumia, E.A. Barboni, R.C. Hughes, NMR solution studies of hamster galectin-3 and electron microscopic visualization of surface-adsorbed complexes: evidence for interactions between the N- and C-terminal domains, Biochemistry 40 (2001) 4859–4866.
[25] T. Funasaka, V. Balan, A. Raz, R.W. Wong, Nucleoporin Nup98 mediates galectin-3 nuclear-cytoplasmic trafficking, Biochem. Biophys. Res. Commun. 434 (2013) 155–161.
[26] S.Y. Li, P.J. Davidson, N.Y. Lin, R.J. Patterson, J.L. Wang, E.J. Arnoys, Transport of galectin-3 between the nucleus and cytoplasm. II. Identification of the signal for nuclear export, Glycobiology 16 (2006) 612–622.
[27] A.B. Yongye, L. Calle, A. Arda, J. Jiménez-Barbero, S. André, H.J. Gabius, K. Martinez-Mayorga, M. Cudic, Molecular recognition of the Thomsen–Friedenreich antigen-threonine conjugate by adhesion/growth regulatory galectin-3: nuclear magnetic resonance studies and molecular dynamics simulations, Biochemistry 51 (2012) 7278–7289.
[28] M. Bartoloni, B.E. Dominguez, E. Dragoni, B. Richichi, M. Fragai, S. André, H.J. Gabius, A. Arda, C. Luchinat, J. Jiménez-Barbero, C. Nativi, Targeting matrix metalloproteinases: design of a bifunctional inhibitor for presentation by tumour-associated galectins, Chem. Eur. J. 19 (2013) 1896–1902.
[29] K. Umemoto, H. Leffler, Assignment of ^{1}H, ^{15}N and ^{13}C resonances of the carbohydrate recognition domain of human galectin-3, J. Biol. NMR 1 (2001) 91–92.